J Appl Physiol 100: 1569–1576, 2006.
First published December 29, 2005; doi:10.1152/japplphysiol.00762.2005.

Oxygen release from arterioles with normal flow and no-flow conditions

Pedro Cabrales,[1] Amy G. Tsai,[1,2] Paul C. Johnson,[1,2] and Marcos Intaglietta[1,2]

[1]*La Jolla Bioengineering Institute, and* [2]*Department of Bioengineering, University of California-San Diego, La Jolla, California*

Submitted 27 June 2005; accepted in final form 26 December 2005

Cabrales, Pedro, Amy G. Tsai, Paul C. Johnson, and Marcos Intaglietta. Oxygen release from arterioles with normal flow and no-flow conditions. *J Appl Physiol* 100: 1569–1576, 2006. First published December 29, 2005; doi:10.1152/japplphysiol.00762.2005.—The rate of oxygen release from arterioles (~55 μm diameter) was measured in the hamster window chamber model during flow and no-flow conditions. Flow was stopped by microvascular transcutaneous occlusion using a glass pipette held by a manipulator. The reduction of the intra-arteriolar oxygen tension (P_{O_2}) was measured by the phosphorescence quenching of preinfused Pd-porphyrin, 100 μm downstream from the occlusion. Oxygen release from arterioles was found to be 53% greater during flow than no-flow conditions (2.6 vs. 1.7 $\times 10^{-5}$ ml $O_2 \cdot cm^{-2} \cdot s^{-1}$, $P < 0.05$). Acute hemodilution with dextran 70 was used to reduce vessel oxygen content, significantly increase wall shear stress (14%, $P < 0.05$), reduce Hct to 28.4% (SD 1.0) [vs. 48.8% (SD 1.8) at baseline], lower oxygen supply by the arterioles (10%, $P < 0.05$), and increase oxygen release from the arterioles (39%, $P < 0.05$). Hemodilution also increased microcirculation oxygen extraction (33% greater than nonhemodilution, $P < 0.05$) and oxygen consumption by the vessel wall, as shown by an increase in vessel wall oxygen gradient [difference in P_{O_2} between the blood and the tissue side of the arteriolar wall, nonhemodiluted 16.2 Torr (SD 1.0) vs. hemodiluted 18.3 Torr (SD 1.4), $P < 0.05$]. Oxygen released by the arterioles during flow vs. nonflow was increased significantly after hemodilution (3.6 vs. 1.8 $\times 10^{-5}$ ml $O_2 \cdot cm^{-2} \cdot s^{-1}$, $P < 0.05$). The oxygen cost induced by wall shear stress, suggested by our findings, may be >15% of the total oxygen delivery to tissues by arterioles during flow in this preparation.

oxygen consumption; occlusion; wall shear stress; arteriolar oxygen exit

THE MICROCIRCULATION AND SYSTEMIC blood vessels are subjected to wall shear stress (WSS), which stimulates the endothelium, mediating many physiological and pathological processes by expressing proteins and factors, which function as vasodilators [e.g., nitric oxide (NO)], vasoconstrictors (e.g., endothelin-1), growth factors (e.g., PDGF), growth inhibitors (e.g., heparin), adhesion molecules (e.g., ICAM-1), and chemoattractants (e.g., monocyte chemotactic protein-1) (7, 12, 13). The biochemical activity attributable to WSS is large, since it involves gene expression, upregulation of protein synthesis, and the moment-to-moment adjustments needed for addressing the microscopic variability of tissue perfusion. The continuous operation of this complex process should require energy expenditure, a process that, at steady-state conditions in living organism, could significantly influence oxygen consumption.

Studies of endothelial cells in vitro report that these cells consume oxygen at a rate that is similar to that of most tissues. As an example, the study of Kjellstrom et al. (19) showed that oxygen consumption of endothelium in cell cultures ranged between 1.6 and 8 $\times 10^{-2}$ ml $O_2 \cdot min^{-1} \cdot g^{-1}$, depending on origin and species. In addition, Motterlini et al. (25) found the value of 5.6 $\times 10^{-2}$ ml $O_2 \cdot min^{-1} \cdot g^{-1}$ for endothelial cells from the pig aorta. However, studies in cell culture may not be representative of in vivo conditions, where the endothelium is in direct contact with smooth muscle and subjected to WSS by the flow of blood, rather than cell culture media.

Oxygen consumption by the endothelium has, until recently, been assumed to be similar to other tissues. However, there is some evidence that it is substantially greater. Measurements in the microcirculation by Tsai et al. (35) showed large oxygen gradients at the microvascular vessel wall, suggesting the use of large amounts of oxygen by the vessel wall. Shibata et al. (30) reached the same conclusion in similar studies. The high rate of oxygen metabolism is supported by the findings of Curtis et al. (9), who determined that an isolated, perfused muscle preparation, denuded of endothelium, consumes about one-third less oxygen than its intact counterpart. Changes in vessel tone have also been shown to significantly increase microvessel oxygen consumption (14, 40).

We propose that WSS stimulates the endothelium to exert a significant biochemical activity, increasing oxygen consumption in vivo when it is present. Conversely, absence of WSS lowers endothelial oxygen consumption. To test this hypothesis, we measured the rate of oxygen release from arterioles in vivo during flow (stimulated by shear stress) and in the absence of flow (lack of shear stress). The rate of oxygen release from arterioles can be determined by the up- and downstream difference in blood P_{O_2} and, therefore, oxygen saturation per unit vessel length times the local flow rate. Occluding the same microvessel by micromanipulation allowed us to measure the rate at which oxygen content within the microvessel decays in the absence of shear stress. Both rates are ultimately determined by the gradient at the blood-vessel wall interface, which is determined by the local diffusion constant and rate of oxygen consumption by the vessel wall and tissue. Since the parenchymal tissue is not affected by changing shear stress, it is plausible to assume that differences in WSS may directly affect the endothelium.

Measurements of the rate of oxygen depletion from blood under flow and no-flow conditions present few uncertainties, since results are directly based on mass balance considerations. In this study, we also measured the rate at which oxygen is released by arterioles during normal flow and oxygen depletion from arterioles upon flow stoppage with normal hematocrit (Hct) and during a 40% normovolemic hemodilution to determine whether altering blood oxygen content affected our results.

Address for reprint requests and other correspondence: P. Cabrales, La Jolla Bioengineering Institute, 505 Coast Blvd. S., Suite 405, La Jolla, CA 92037 (e-mail: pcabrales@ucsd.edu).

The costs of publication of this article were defrayed in part by the payment of page charges. The article must therefore be hereby marked "*advertisement*" in accordance with 18 U.S.C. Section 1734 solely to indicate this fact.

METHODS

Animal Preparation

Investigations were performed in 55- to 65-g golden Syrian hamsters (Charles River Laboratories, Boston, MA). Animal handling and care were provided following the procedures outlined in the Guide for the Care and Use of Laboratory Animals (National Research Council, 1996). The study was approved by the local Animal Use Committee. The hamster window chamber model is widely used for microvascular studies without anesthesia (awake model), and the complete surgical technique is described in detail elsewhere (8, 11). Briefly, the animal was prepared for chamber implantation with a 50 mg/kg ip injection of pentobarbital sodium as anesthesia. After hair removal, sutures were used to lift the dorsal skin away from the animal, and one frame of the chamber was positioned on the animal's back. A chamber consisted of two identical titanium frames with a 15-mm circular window. One side of the skin fold was removed with the aid of backlighting and a stereomicroscope following the outline of the window, until only a thin layer of retractor muscle and the intact subcutaneous skin of the opposing side remained. Saline and then a cover glass were placed on the exposed skin that was held in place by the other frame of the chamber. The intact skin of the other side was exposed to the ambient environment. The animal was allowed at least 2 days for recovery; then its chamber was assessed under the microscope for any signs of edema, bleeding, or unusual neovascularization. Barring these complications, the animal was anesthetized again with pentobarbital sodium. Arterial and venous catheters (PE-50) were implanted in the carotid artery and jugular vein. The catheters were filled with a heparinized saline solution (30 IU/ml) to ensure their patency at the time of experiment. Catheters were tunneled under the skin and exteriorized at the dorsal side of the neck, where they were attached to the chamber frame with tape. The experiment was performed between 24 and 48 h after catheter implantation.

Inclusion Criteria

Animals were suitable for the experiments if systemic parameters were within normal range for Golden Syrian hamsters (6, 29), namely, heart rate (HR) $>$ 340 beat/min, mean arterial pressure (MAP) $>$ 80 mmHg, systemic Hct $>$ 45%, and arterial oxygen partial pressure (Pa_{O_2}) $>$ 50 Torr. The comparatively low Pa_{O_2} and high P_{CO_2} of these animals are a consequence of their adaptation to a fossorial environment (6, 29).

Systemic Parameters and Blood-Gas Parameters

MAP was continuously monitored, and the HR was determined from the pressure trace. Arterial blood was collected in heparinized glass capillaries (0.05 ml) and immediately analyzed for P_{O_2}, P_{CO_2}, base excess, and pH (Blood Chemistry Analyzer 248, Bayer, Norwood, MA). A second capillary tube was used for Hct measurement. Hb content was determined spectrophotometrically with a single drop of blood (B-Hemoglobin, Hemocue, Stockholm, Sweden).

Microhemodynamic Parameters

Detailed mappings of the vasculature were made so that the same vessels were studied throughout the experiment. Arterioles (50- to 65-μm diameter and 0.5- to 1-mm length and devoid of branching) were chosen, according to their visual clarity.

Blood flow velocity was measured online using the photodiode cross-correlation technique (16) (Fiber Optic Photo Diode Pickup and Velocity Tracker Model 102B; Vista Electronics, San Diego, CA). The video image shearing technique was used to measure vessel diameter (D) online (24). Automated diameter measurements were obtained by first spatially differentiating the image elements, thus creating a pseudovascular wall whose separation was measured by an edge-detection algorithm, previously calibrated in situ with the image-shearing monitor. The measured centerline velocities (v) were corrected according to vessel size to obtain the mean red blood cell (RBC) velocity V (18). Blood flow ($\dot{Q}$) was calculated from the measured parameters as $\dot{Q} = V \times \pi\ (D/2)^2$. WSS was defined by $WSS = WSR \times \eta$, where WSR is the wall shear rate given by $8VD^{-1}$, and η is either whole blood viscosity (WSS_B), plasma viscosity (WSS_P), or the viscosity of blood at the level of arterioles. According to Lipowsky and Firrell (22), Hct in arterioles is 58% of the systemic value and is 70% of the systemic value in hemodilution when Hct is ~30%. Therefore, we corrected our hemodilution viscosity by calculating the local Hct and then using the corresponding viscosity obtained from actual viscosity vs. Hct data from dilutions of hamster blood (4).

Microvascular P_{O_2} Measurements

High-resolution microvascular P_{O_2} measurements were made using phosphorescence quenching microscopy, described in detail elsewhere (33, 39), which was implemented, according to the description of Kerger et al. (18). Oxygen measurements are based on oxygen-dependent quenching of phosphorescence emitted by an albumin-bound metalloporphyrin complex after pulsed light excitation. Animals received a slow intravenous injection of palladium-meso-tetra (4-carboxyphenyl) porphyrin (15 mg/kg body wt at 10 mg/m; Porphyrin Products, Logan, UT). The dye circulated for 10 min before P_{O_2} measurements. An optical window of 20 × 5 μm placed longitudinally along the blood vessel allows us to locate the measuring site. Measurements in normal flow conditions used the phosphorescence of 10 excitation flashes delivered at a rate of 10 flashes/s. Measurements during occlusion were made every second using a single flash. Tissue was also the average phosphorescence of 10 excitation flashes delivered at a rate of 10 flashes/s. Flash intensity and duration (5 μs) were the same for both determinations (35).

Arteriolar Occlusions

The arterioles were occluded with a glass micropipette made with 1-mm-diameter glass tubing whose tip is drawn into a long fiber by a pipette puller (P-87 horizontal puller, Sutter Instruments, Novato, CA). The fiber was bent over a flame, and the knee of the bend was pressed on the intact skin of the preparation mounted on an inverted microscope that allowed the observation of the opposite side of the window chamber, i.e., the intact microcirculation (Fig. 1). Additionally, diameter was also measured continuously during the occlusion period from video recordings to ensure preservation of flow conditions. The objective of this experiment was to determine the rate at which oxygen exits the arterioles, which preliminary trials showed to reach completion (~4 mmHg) within 15 s from the time of occlusion; therefore, more extended periods of occlusion were not investigated.

Experimental Setup and Protocol

The unanesthetized animal was placed in a restraining tube and stabilized under the microscope. Microvessels were observed by transillumination with an inverted microscope (IMT-2 Olympus, New Hyde Park, NY) using a ×20 objective (0.7 numerical aperture, Olympus). Arteriolar microocclusion was performed as previously described (29). Once an arteriole had been selected for measurement, the microoccluder was positioned between the intact skin and the optics of the substage illumination. The tip of the occluder was placed near the center of the optical field of view, and the vessel was similarly placed using the stage micrometric position controls. The occluder was moved against the vessel, compressing an area of ~50 μm in diameter; occlusion was sustained for a period of 30 s.

Acute Isovolemic Hemodilution

Progressive hemodilution to a final systemic Hct level of 60% of baseline was accomplished with an isovolemic exchange with dextran

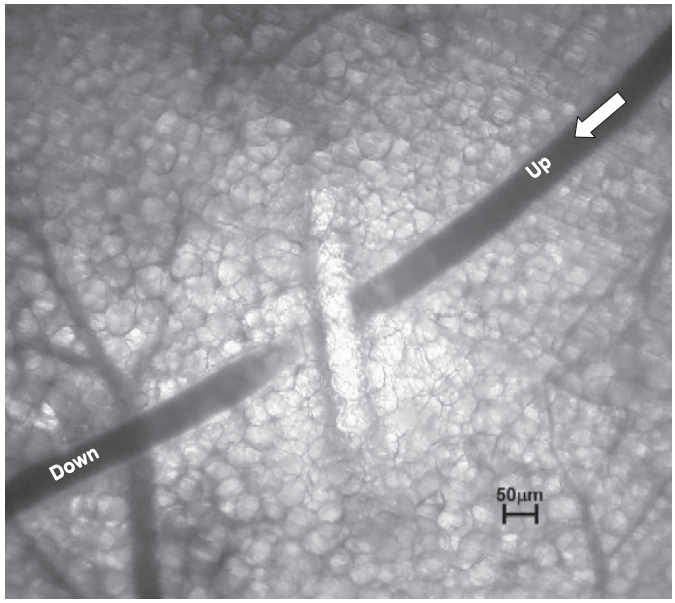

Fig. 1. Microphotograph of an occluded arteriole in the hamster window chamber. The glass fiber lies across the arteriole. The arteriole is visualized through the glass coverslip, and the occluder is positioned by trial and error against the opposite side of the chamber against the normal skin by means of a micromanipulator. Pressing the occluder against the skin compresses a circular area of ~50 μm diameter and occludes the vessel. Arrow indicates flow direction.

70 (molecular weight = 70,000; B. Braun, Irvine, CA). This protocol was described in detail before (5, 6, 34). Briefly, the volume of the exchange-dilution step was calculated as 40% of the blood volume, with the latter estimated as 7% of the body weight. Results were compared with baseline values before hemodilution. The dextran 70 solution was infused into the jugular vein catheter after passing through an inline, 13-mm-diameter, 0.2-μm syringe filter at a rate of 100 μl/min. Blood was simultaneously withdrawn by a dual syringe pump ('33' syringe pump, Harvard Apparatus, Holliston, MA) at the same (isovolemic-normovolemic) rate from the carotid artery catheter (5, 34, 36). This slow rate of exchange provided for a stable MAP immediately after the exchange. A 10-min stabilization period was allowed before data acquisition.

Oxygen Exit from Vessels with Flow

The rate of oxygen exit from vessels with flow ($J_{O_2\ convection}$) was determined from the difference in oxygen content between upstream ($[O_2]_{upstream}$) and downstream ($[O_2]_{downstream}$) locations and the flow rate ($\dot{Q}$) of blood in the vessel segment, according to the equation:

$$J_{O_2\ convection} = \dot{Q}([O_2]_{upstream} - [O_2]_{downstream})/A_s \quad (1)$$

where the oxygen content of blood $[O_2] = C_b\ [f\ HCT]So_2$, where C_b is oxygen binding capacity of blood; [*f* HCT] is the ratio of microvascular to systemic Hct, a function of vessel diameter (17, 26), and physically dissolved O_2 is neglected because of low solubility of O_2 in plasma; and So_2 is HbO_2 saturation determined from the measurement of intravascular Po_2 and converted to So_2 from measurements of the oxygen dissociation curve of hamster blood using a Hemox analyzer (TCS Scientific, New Hope, PA). This instrument uses dual-wavelength spectrophotometry to calculate Hb saturation while measuring the dissolved oxygen concentration with a Clark oxygen electrode. A_s is the inner vessel wall surface area between the upstream and downstream Po_2 measurement locations. This calculation assumes that systemic blood pH and microcirculation pH are similar and invariant during occlusion, an assumption verified for pH in a different study (3).

Oxygen Release From Vessels with No Flow

The rate of oxygen exit per unit vessel wall area from the occluded arterioles ($J_{O_2\ occlusion}$) (no shear stress) was calculated by measuring the rate of decrease in oxygen content from the occluded vessel according to:

$$J_{O_2\ occlusion} = C_b[f\mathrm{HCT}](dSo_2/dt)(\mathrm{Vol}/A_s) \quad (2)$$

where dSo_2/dt is the slope of the curve of O_2 saturation of Hb corresponding to the measured Po_2 during the occlusion, according to our measurements of the oxygen dissociation curve of hamster blood; and $\mathrm{Vol}/A_s = D/4$ is the ratio between volume ($\pi D^2 l/4$, where *d* is the diameter and *l* is the vessel segment length) and wall vessel surface area $A_s = \pi Dl$. It should be noted that calculations of oxygen release are relative to the oxygen content of the same vessel. Therefore, the actual Hct in the vessels is not as critical as determining the rates at which oxygen is depleted from the vessels, during flow and nonflow conditions, since there should be no difference in vessel Hct between the two conditions.

Data Analysis

Results are presented as means and SD. Microvascular hemodynamic data are presented as absolute values. Oxygen data are presented as ratios relative to baseline values before occlusion. A ratio of 1.0 signifies no change from baseline, whereas lower and higher ratios are indicative of changes proportionally higher and lower than baseline. For repeated measurements, time related changes were assessed by analysis of variance. Comparisons between different groups of animals were performed with the Wilcoxon signed rank test (GraphPad Prism 4.01; GraphPad Software, San Diego, CA). Changes were considered statistically significant if $P < 0.05$.

RESULTS

Fifteen animals were studied, providing data for 70 arteriolar vessels: 45 during normal flow conditions (25 baseline and 20 after hemodilution), and 25 during microvessel occlusion (15 baseline and 10 after hemodilution). The systemic parameters (MAP, HR, Pa_{O_2}, arterial Pco_2, base excess, and pH) were not statistically changed after hemodilution. Acute hemodilution with dextran 70 decreased oxygen-carrying capacity, as Hct was reduced from 48.8 (SD 1.8) to 28.4% (SD 1.0) and Hb from 15.1 (SD 0.7) to 8.9 g Hb/dl (SD 0.5). Systemic parameters are presented in Table 1.

Table 1. *Macrohemodynamic parameters before and after hemodilution*

	Baseline	Hemodilution
n	10	5
Hct, %	48.8 (1.8)	28.4 (1.0)*
Hb, g/dl	15.1 (0.7)	8.9 (0.5)*
MAP, mmHg	98.9 (8.1)	94.7 (7.2)
Heart rate, beats/min	434.5 (44.7)	456.6 (33.8)
Pa_{O_2}, Torr	59.8 (5.5)	65.8 (6.2)
Pa_{CO_2}, Torr	52.8 (4.1)	49.2 (5.6)
Arterial pH	7.34 (0.02)	7.35 (0.02)
Base excess, mmol/l	3.2 (1.2)	2.9 (1.0)
Blood viscosity, cP	4.2	2.8
Plasma viscosity, cP	1.2	1.3

Values are means (SD); *n,* no. of animals. Baseline included all of the animals in the study. Hct, systemic hematocrit; Hb, hemoglobin content of blood; MAP, mean arterial blood pressure; Pa_{O_2}, arterial partial O_2 pressure; Pa_{CO_2}, arterial partial pressure of CO_2. *$P < 0.05$, compared with baseline.

Table 2. *Microhemodynamic parameters before and after hemodilution*

	Baseline	Hemodilution
n	46	24
Diameter, μm	58.3 (4.8)	56.8 (5.1) [0.96 (0.05)]
Centerline velocity, mm/s	5.3 (1.4)	6.9 (1.5)* [1.57 (0.14)]
Mean flow, nl/s	9.3 (3.1)	11.4 (3.8)* [1.26 (0.17)]
WSR, s^{-1}	698 (97)	1,007 (142)*[1.44 (0.18)]
WSS_B, dyn/cm^2	29.3 (4.1)	28.2 (4.0) [0.97 (0.12)]
WSS_P, dyn/cm^2	8.4 (1.2)	13.1 (1.8)* [1.56 (0.19)]
WSS_M, dyn/cm^2	19.5 (2.8)	22.1 (3.2)* [1.14 (0.11)]

Values are means (SD); *n,* no. of animals. WSR, calculated wall shear rate; WSS, calculated wall shear stress (subscript B, blood viscosity; P, plasma viscosity; M, microcirculation viscosity). In brackets are pairwise comparisons. *$P < 0.05$: compared with baseline.

Microhemodynamic Changes After Hemodilution

Diameter decreased from 58.3 (SD 4.8) to 56.8 μm (SD 5.1) [0.96 (SD 0.05) of baseline] after hemodilution ($P = 0.31$). Center RBC velocity increased statistically significantly from 5.3 (SD 1.4) to 6.9 μm (SD 1.5) [1.57 (SD 0.14) of baseline] after hemodilution ($P < 0.05$). Calculated mean arteriolar flow increased statistically significantly from 9.3 (SD 3.1) to 11.4 μm (SD 3.8) [1.26 (SD 0.17) of baseline] after hemodilution ($P < 0.05$). Measured and calculated hemodynamic parameters are presented in Table 2.

Intravascular and Tissue Oxygen

Arteriolar oxygen levels increased significantly from 50.9 (SD 4.3) to 55.4 mmHg (SD 4.7) after hemodilution ($P < 0.05$) (Table 3). Tissue P_{O_2} was not affected by hemodilution ($n = 24$, sites at baseline and after hemodilution). Venular oxygen decreased significantly from 34.2 mmHg (SD 3.1) ($n = 22$) to 29.4 mmHg (SD 3.0) ($n = 20$) after hemodilution ($P < 0.05$). This microvascular distribution of P_{O_2} values is essentially the same as that found in the hamster in baseline conditions.

Oxygen Exit From Vessels During Flow

The rate of oxygen exit from vessels with flow (vessel subjected to WSS) was 2.6×10^{-5} ml $O_2 \cdot cm^{-2} \cdot s^{-1}$ (SD 0.6)for baseline (normal Hct) and significantly increased to 3.6×10^{-5} ml $O_2 \cdot cm^{-2} \cdot s^{-1}$ (SD 0.7) for the hemodiluted condition ($P < 0.05$) (Table 4). The vessel wall gradient was statistically significant different for baseline [16.2 mmHg (SD 1.0)] compared with hemodilution [18.3 mmHg (SD 1.4), $P < 0.05$].

Table 3. *Oxygen levels*

	Baseline	Hemodilution
Arteriolar, mmHg	50.9 (4.3)	55.4 (4.7)*
HbO_2 saturation, %	81.3 (2.7)	83.5 (2.6)*
Venular, mmHg	34.2 (3.1)	29.4 (3.0)*
HbO_2 saturation, %	54.6 (4.2)	43.6 (4.0)*
Tissue, mmHg	22.8 (2.2)	21.7 (2.9)
Wall O_2 gradient, mmHg	16.2 (1.0)	18.3 (1.4)*
Saturation A-V difference, %	25.6 (2.1)	39.6 (2.6)*
O_2 supply, 10^{-6} ml O_2/min	53.7 (2.7)	48.1 (2.4)*
O_2 release, 10^{-6} ml O_2/min	16.4 (1.7)	21.8 (1.4)*

Values are means (SD). A-V, arteriovenous. *$P < 0.05$: compared with baseline.

Table 4. *Arteriolar oxygen release levels*

	Baseline	Hemodilution
Flow		
P_{O_2} upstream, Torr	51.8 (1.4)	55.9 (1.7)*
HbO_2 saturation, %	81.1 (1.8)	83.9 (1.7)*
P_{O_2} downstream, Torr	48.1 (1.1)	48.7 (1.5)
HbO_2 saturation, %	77.5 (1.6)	78.1 (1.6)
Diameter, μm	57.2 (3.1)	55.7 (2.9)
Centerline velocity, mm/s	5.1 (1.4)	6.5 (1.6)*
Mean flow, nl/s	7.9 (2.0)	9.8 (2.2)*
O_2 exit, 10^{-5} ml $O_2 \cdot cm^{-2} \cdot s^{-1}$	2.6 (0.6)	3.6 (0.7)*
Occlusion		
P_{O_2} upstream, Torr	50.9 (1.6)	55.4 (1.9)*
HbO_2 saturation, %	80.3 (1.3)	83.7 (1.4)*
Diameter, μm	57.4 (2.8)	56.9 (2.8)
Time, s	12.8 (1.0)	7.8 (0.8)*
O_2 exit, 10^{-5} ml $O_2 \cdot cm^{-2} \cdot s^{-1}$	1.7 (0.4)†	1.8 (0.5)†

Values are means (SD); flow: $n = 25$ for baseline and $n = 20$ for hemodilution; occlusion: $n = 15$ for baseline and $n = 10$ for hemodilution. $P < 0.05$ compared with *baseline and †flow.

Diameter Changes During Occlusion

Diameter tended to decrease slightly during occlusion, an effect that was most apparent 30 s after occlusion, although not statistically significant (slight constriction 4.6%, $P = 0.21$). Oxygen exit during occlusion was extrapolated to the zero time of occlusion, with arteriolar oxygen depletion being estimated using the diameter of the location measured during flow conditions.

Oxygen Release from Vessels with No Flow

The decrease of blood P_{O_2} as a function of time in the occluded vessels is shown in Fig. 2*A* for normal and hemodiluted vessels. These rates were statistically different at 3.57 (SD 0.36) and 4.11×10^{-5} ml $O_2 \cdot cm^{-2} \cdot s^{-1}$ (SD 0.49), respectively ($P < 0.05$). These values were computed estimating the slope of P_{O_2} vs. time immediately following occlusion. The rates of oxygen depletion from the occluded vessels were 12.8 s (SD 1.0) at baseline and 7.8 s (SD 0.8) after hemodilution ($P < 0.05$).

Oxygen release could only be measured on the downstream side of the occlusion. Conditions on the upstream side were strongly influenced by the arterial pressure pulse, which caused perturbations in the occluded region, inducing significant mixing that was evidenced by the motion of RBCs. Consequently, the P_{O_2} measured upstream from the occlusion remained consistent during the occlusion. Figure 2*A* shows the rapid decline of intravascular P_{O_2} in the downstream side of the occluded vessels with both baseline (normal Hct) and hemodilution. Data were obtained at ~100 μm from the point of occlusion, because this location consistently yielded the lowest value of intravascular tissue P_{O_2} when intravascular and tissue oxygen equilibrated. Locations further downstream from the center of occlusion showed an initial decrease in intravascular P_{O_2} that stabilized at a value higher than that measured at the 100-μm location after 15–20 s from the instant of occlusion (due to

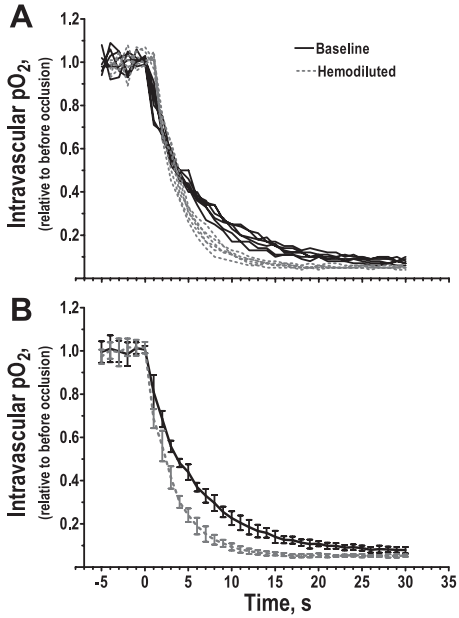

Fig. 2. Decay of intravascular P_{O_2} after the occlusion of arterioles. The solid line corresponds to blood vessels at baseline (normal Hct), and the dotted line corresponds to arterioles of animals subjected to a 40% Hct reduction by hemodilution. *A*: examples of individual P_{O_2} values normalized to the intravascular P_{O_2} value measured at the same location before occlusion. *B*: the average and SD of the data in *A*. *Time 0* corresponds to the occlusion point.

diffusion from the perfused outer boundary of the occlusion zone).

DISCUSSION

The principal finding of this study is that the rate of oxygen exit from arterioles was ~53% higher during flow than no-flow (occluded) conditions for baseline (nonhemodiluted) and 100% higher during flow vs. no flow after acute hemodilution. See Figure 3. Differences in oxygen exit between flow and no-flow conditions do not appear to be related to total oxygen content, as presented by the result with the two Hct values studied. Furthermore, significantly more oxygen was released from arterioles during hemodilution (38%) than during flow, probably introduced by the increase in WSR after hemodilution (WSR being calculated on the basis of either plasma or local blood viscosity).

The rheological properties of blood (RBCs and plasma) at the adjacent space to the vessel wall, "plasma layer," that causes fluid shear on the luminal endothelial-cell surface can only be establish by microfluidics, and the use of plasma and local viscosity to calculate WSS are the most accurate approximation from macroscopic measurements. WSS calculated using plasma or local blood viscosity is a realistic assessment of local WSS, since the change in Hct, and therefore viscosity in the microcirculation, is well established (22, 23). Using plasma viscosities, WSS yielded a 56% increase after hemodilution (Table 2), and using the estimated local blood viscosity the increase was 14%. There was no statistically significant difference in the rate of oxygen depletion from occluded arterioles between baseline (normal Hct) and hemodilution. Since this latter finding corresponds to WSS being identical and zero in both groups of vessels, this finding supports the hypothesis that shear stress influences oxygen release into the tissues.

Acute hemodilution caused less oxygen to be delivered to the microcirculation, as shown in Table 3. In contrast, oxygen extraction in the microcirculation and presumably consumption was statistically significantly increased by 33% relative to baseline. This increased oxygen extraction during hemodilution is similar to the significantly increased oxygen release from arterioles (38%). Because tissue P_{O_2} was the same for baseline and hemodilution and extraction increased, it appears that hemodilution increases oxygen consumption by the tissue. Considering the proposed link between wall gradient and oxygen consumption found in other studies (14, 15, 30, 35), the present findings where wall oxygen gradient was significantly increased from baseline after hemodilution suggest that increased oxygen extraction in hemodilution is due to an increased wall oxygen consumption.

Analysis of Factors Affecting Calculations

Considering all of the settings and measurements that determine the experimental results, the following errors may affect the calculated parameter.

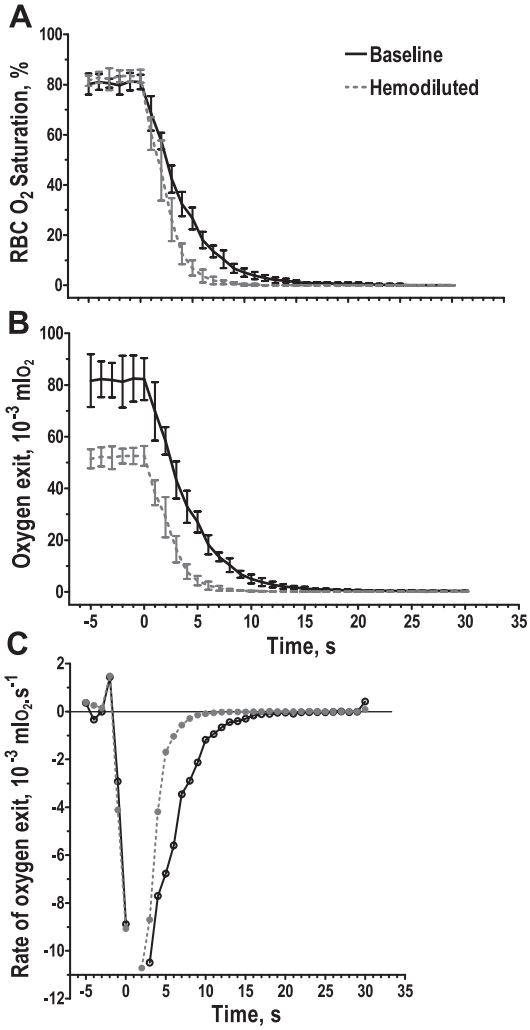

Fig. 3. Decay of intravascular oxygen after the occlusion of arterioles. The solid line corresponds to blood vessels at baseline (normal Hct), and the dotted line corresponds to arterioles of animals subjected to a 40% Hct reduction by hemodilution. *A*: red blood cell (RBC) saturation corresponding to the data in Fig. 2*B*. *B*: oxygen content in occluded vessel. *C*: rate of oxygen exit after occlusion. *Time 0* corresponds to the occlusion point.

Flow calculation. Correction factor for the measured RBC centerline velocity affects the calculation of mean blood flow and the rate of oxygen released by the arterioles. Experimental studies of blood flow in glass tubes of 15- to 80-μm internal diameter, using human RBCs with the dual-slit system (1, 24), show that the centerline velocity measured by the dual-slit method is 80% of the true centerline velocity. Therefore, since parabolic flow profile centerline velocity is two times the average velocity, the actual average flow velocity is 0.625 times (1/1.6) the measured centerline velocity. This relationship holds true within 5–10% over a wide range of flow velocities (0.5–27.0 mm/s), according to Lipowsky and Zweifach (24) and for Hct in the range of 6–60% in tubes above 40-μm diameter (1). The factor 0.625 (1/1.6) increases and becomes 1.00 for velocities measured with the photodiode cross-correlation technique in capillaries, i.e., when the velocity profile may be considered to be uniform across the vessel lumen. The studies that determined the 0.625 value were carried out in glass tubes, where average flow velocity could be measured by two independent means. In these studies, blood was heparinized, lowering interaction between blood elements, yielding the parabolic profile assumed for the calculation of this coefficient. The coefficient was verified in vivo by Proctor et at. (27), and LaLone and Johnson (21) found agreement between calculated volume flow in an arteriole at wide and narrow segments of the vessels. The same was true of the sum of flows of daughter vessels at branch points compared with flow in the feeding vessel. On the other hand, if the velocity profile is blunted according to recent evidence (31, 32), then the average flow velocity is greater than one-half of the centerline velocity, and the 0.625 factor is increased. Therefore, the calculated flow for the arterioles under consideration may underestimate flow and the rate of oxygen release from the arterioles during flow.

Intravascular P_{O_2} measurements. Oxygen measurements were performed at the centerline of the blood vessels. Therefore, there should be no methodical difference between measurements during flow vs. nonflow conditions, since illumination is the same. The fact that there may be a slight constriction (on the order of 5%, $P = 0.21$) of vessel diameter, not statistically significant, which develops in time and becomes evident ~30 s after occlusion, would increase the surface-to-volume ratio, and, therefore, the rate of oxygen exit, thus overestimating this phenomenon during nonflow conditions. Another source of error could be due to oxygen consumption by the measuring method. This was shown by Tsai et al. (35) to be 0.02 mmHg per excitation flash in tissue. Since measurements were done in blood, where oxygen concentration is ~10 times greater, using 10 flashes per measurement, the lowering of blood P_{O_2} due to oxygen consumption is ~0.02 Torr per measurement. Forty P_{O_2} measurements in the occluded vessels were carried out for each determination, potentially reducing the measured P_{O_2} by 1 Torr. As in the previous case, this source of error may overestimate the rate of oxygen exit from the occluded arteriole. Therefore, measurements in flowing blood vessels may underestimate the rate of oxygen exit from the arterioles, while those in the occluded vessel tend to overestimate oxygen exit. It appears that the actual discrepancy in oxygen release between flow and no-flow conditions may be greater and not due to methodological errors.

Plasma layer thickness. During flow conditions, an RBC-free plasma layer develops at the blood tissue interface due to axial migration (38). In stop-flow conditions, hydrodynamic effects are no longer present, and the plasma layer should disappear. The presence of this plasma layer poses a resistance to the diffusion of oxygen that is partly mitigated by the radial dispersion in the trajectory of RBCs near the vessel wall. According to the studies of Diller and Mikic (10), this causes shear-induced particle diffusion and the increase of the effective diffusion coefficient of oxygen. However, changes in the diffusion for oxygen were not seen in the study of Briceño et al. (2), who found that the oxygen profiles in arterioles were essentially identical to those predicted by Kobayashi et al. (20), based on the analysis of oxygen transfer in blood in laminar flow in the absence of shear augmented diffusion. Our results, however, show that the rate of oxygen release from blood is greater during flow (presumably when the plasma layer is present) than with no flow, when the plasma layer is no longer present.

Diffusion constants. The rate of oxygen release from arterioles is due to diffusion, which is governed by the diffusion constant and the oxygen concentration gradient. The diffusion resistance regulating arteriolar oxygen exit should be the same or greater during flow conditions due to the presence of the plasma layer. The remaining factor that can account for the difference in oxygen release from the arterioles during flow vs. no flow is the presence of an increased oxygen concentration gradient along the diffusion path. Since the geometry of the system is identical for both conditions, a remaining possibility is that the diffusion gradient is increased during flow due to increased oxygen consumption in the endothelium (vessel wall exposed to the effects of shear stress).

Arteriolar Wall and Oxygen Consumption

The arteriolar wall is a significant oxygen sink, according to recent studies (35, 37), whose rate of oxygen consumption can be modulated by vasoactive materials (14, 15). Shear stress is a major stimulus of endothelial cells, which respond rapidly and sensitively to the mechanical phenomena induced by blood flow (12, 13). NO, prostacyclin, and endothelin-1 are end products of this process, which, furthermore, involves activation and deactivation of genes, protein expression, and a multitude of biochemical events that presumably require energy and oxidative metabolism to proceed.

Shear stress modulates endothelial mechanosensors that trigger phosphorylation cascades of signaling molecules of intracellular pathways, causing the production of transcription factors, and the expression of genes and proteins stimulates cytoskeletal alignment and cell shape and changes ion conductances. It governs NO synthase and the production of NO and prostacyclin. These responses occur within seconds to hours of the imposition of changes in shear stress in cells cultured under dynamic conditions (7). However, they are generally not investigated in cell cultures where smooth muscle is also present, and a significant component of oxygen consumption by the vessel wall may be related to the interaction of these cellular species in vivo.

Sudden flow cessation in arterioles causes a rapid depletion of intravascular oxygen. The occluded vessel, near the occlusion, reaches intravascular P_{O_2} values of 3–4 Torr in ~15 s.

Similar levels were found by Richmond et al. (28), who occluded the arterial supply of exposed skeletal muscle and found that oxygen was depleted from the tissue in ~15 s. Tissue P_{O_2} never reached zero after occlusion, probably due to oxygen diffusion from surrounding tissue and other vessels.

In conclusion, oxygen release from arterioles in the intact tissue of unanesthetized animals is significantly greater during flow conditions compared with the oxygen rate of exit from mechanically occluded vessels. Analysis of the potential errors tends to underestimate the release of oxygen during flow and overestimate the release of oxygen during no flow, suggesting that our result is not an artifact related to the experimental methodology. The increased oxygen exit from arterioles could be related to the difference in shear stress between flow and no-flow conditions, since shear stress induces a significant oxidative metabolic activity in the endothelium, which requires oxygen. Hemodilution shows increased shear stress relative to baseline, increased oxygen exit from arterioles during flow, increased oxygen release from the microcirculation to the tissue, and possibly increased oxygen consumption by the vessel wall (increased vessel wall gradient). Considering that the arterioles in some tissues supply as much or more oxygen than capillaries (37) and that the difference in oxygen delivery from arterioles between flow and no-flow conditions is >30%, it would appear that the oxygen cost of shear stress-induced oxygen consumption suggested by our findings may be >15% of oxygen delivery by arteriolar flow in our tissue model. However, the relative significance of the vessel wall as an oxygen sink due to an increase in metabolic activity cannot be assessed at this time. Investigations at a reduced Hct and increased vessel wall stress show a 100% difference in oxygen delivery from arterioles, with and without shear stress, in the absence of changes of tissue P_{O_2}. This further supports the hypothesis that shear stress is a factor in endothelium/vessel wall oxygen consumption.

GRANTS

This work was supported by National Heart, Lung, and Blood Institute Bioengineering Research Partnership Grant R24-HL-64395 and Grants R01-HL-62354 and R01-HL-62318 to M. Intaglietta.

REFERENCES

1. **Baker M and Wayland H.** On-line volume flow rate and velocity profile measurement for blood in microvessels. *Microvasc Res* 7: 131–143, 1974.
2. **Briceño JC, Cabrales P, Tsai AG, and Intaglietta M.** Radial displacement of red blood cells during hemodilution and the effect on arteriolar oxygen profile. *Am J Physiol Heart Circ Physiol* 286: H1223–H1228, 2004.
3. **Cabrales P, Intaglietta M, and Tsai AG.** Early difference in tissue pH and microvascular hemodynamics in hemorrhagic shock resuscitation using peg-albumin and hydroxyethyl starch based plasma expanders. *Shock* 24: 66–73, 2005.
4. **Cabrales P, Tsai AG, Frangos JA, Briceno JC, and Intaglietta M.** Oxygen delivery and consumption in the microcirculation after extreme hemodilution with perfluorocarbons. *Am J Physiol Heart Circ Physiol* 287: H320–H330, 2004.
5. **Cabrales P, Tsai AG, and Intaglietta M.** Alginate plasma expander maintains perfusion and plasma viscosity during extreme hemodilution. *Am J Physiol Heart Circ Physiol* 288: H1708–H1716, 2005.
6. **Cabrales P, Tsai AG, and Intaglietta M.** Microvascular pressure and functional capillary density in extreme hemodilution with low and high plasma viscosity expanders. *Am J Physiol Heart Circ Physiol* 287: H363–H373, 2004.
7. **Chien S, Li S, and Shyy YJ.** Effects of mechanical forces on signal transduction and gene expression in endothelial cells. *Hypertension* 31: 162–169, 1998.
8. **Colantuoni A, Bertuglia S, and Intaglietta M.** Quantitation of rhythmic diameter changes in arterial microcirculation. *Am J Physiol Heart Circ Physiol* 246: H508–H517, 1984.
9. **Curtis SE, Vallet B, Winn MJ, Caufield JB, King CE, Chapler CK, and Cain SM.** Role of vascular endothelium in O_2 extraction during progressive ischemia in canine skeletal muscle. *J Appl Physiol* 79: 1351–1360, 1995.
10. **Diller TE and Mikic BB.** Oxygen diffusion in blood: a translational model of shear induced augmentation. *J Biomech Eng* 105: 67–72, 1980.
11. **Endrich B, Asaishi K, Götz A, and Messmer K.** Technical report: A new chamber technique for microvascular studies in unanaesthetized hamsters. *Res Exp Med (Berl)* 177: 125–134, 1980.
12. **Frangos JA, Eskin SG, McIntire LV, and Ives CL.** Flow effects on prostacyclin production in cultured human endothelial cells. *Science* 227: 1477–1479, 1985.
13. **Frangos JA, Huang TY, and Clark CB.** Steady shear and step changes in shear stimulate endothelium via independent mechanisms—superposition of transient and sustained nitric oxide production. *Biochem Biophys Res Commun* 224: 660–665, 1996.
14. **Friesenecker B, Tsai AG, Dunser MW, Mayr AJ, Martini J, Knotzer H, Hasibeder W, and Intaglietta M.** Oxygen distribution in the microcirculation following arginine-vasopressin induced arteriolar vasoconstriction. *Am J Physiol Heart Circ Physiol* 287: H1792–H1800, 2004.
15. **Hangai-Hoger N, Tsai AG, Friesenecker B, Cabrales P, and Intaglietta M.** Microvascular oxygen delivery and consumption following treatment with verapamil. *Am J Physiol Heart Circ Physiol* 288: H1515–H1520, 2005.
16. **Intaglietta M, Silverman NR, and Tompkins WR.** Capillary flow velocity measurements in vivo and in situ by television methods. *Microvasc Res* 10: 165–179, 1975.
17. **Kanzow G, Pries AR, and Gaehtgens P.** Analysis of the hematocrit distribution in the mesenteric microcirculation. *Int J Microcirc Clin Exp* 1: 67–79, 1982.
18. **Kerger H, Groth G, Kalenka A, Vajkoczy P, Tsai AG, and Intaglietta M.** P_{O_2} measurements by phosphorescence quenching: characteristics and applications of an automated system. *Microvasc Res* 65: 32–38, 2003.
19. **Kjellstrom BT, Ortenwall P, and Risberg R.** Comparison of oxidative metabolism in vitro in endothelial cells from different species and vessels. *J Cell Physiol* 132: 578–580, 1987.
20. **Kobayashi H, Takizawa N, Negishi T, and Tanishita K.** Intravascular inhomogeneous oxygen distribution in microvessels: theory. *Resp Physiol Neurobiol* 133: 271–275, 2002.
21. **LaLone BJ and Johnson PC.** Estimation of arteriolar volume flow from dual-slit red cell velocity: an in vivo study. *Microvasc Res* 16: 327–339, 1978.
22. **Lipowsky HH and Firrell JC.** Microvascular hemodynamics during systemic hemodilution and hemoconcentration. *Am J Physiol Heart Circ Physiol* 250: H908–H922, 1986.
23. **Lipowsky HH, Usami S, and Chien S.** In vivo measurements of apparent viscosity and microvessel hematocrit in the mesentery of the cat. *Microvasc Res* 19: 297–310, 1980.
24. **Lipowsky HH and Zweifach BW.** Application of the "two-slit" photometric technique to the measurement of microvascular volumetric flow rates. *Microvasc Res* 15: 93–101, 1978.
25. **Motterlini R, Kerger H, Green CJ, Winslow RM, and Intaglietta M.** Depression of endothelial and smooth muscle cell oxygen consumption by endotoxin. *Am J Physiol Heart Circ Physiol* 275: H776–H782, 1998.
26. **Pries AR, Secomb TW, Sperandio M, and Gaehtgens P.** Blood flow resistance during hemodilution: effect of plasma composition. *Cardiovasc Res* 37: 225–235, 1998.
27. **Proctor KG, Damon DN, and Duling BR.** Inaccuracies in blood flow estimates in microvessels during arteriolar vasoconstriction. *Microvasc Res* 28: 23–36, 1984.
28. **Richmond KN, Shonat RD, Lynch RM, and Johnson PC.** Critical P_{O_2} of skeletal muscle in vivo. *Am J Physiol Heart Circ Physiol* 277: H1831–H1840, 1999.
29. **Sakai H, Cabrales P, Tsai AG, Tsuchida E, and Intaglietta M.** Oxygen release from low and normal P50 Hb-vesicles in transiently occluded arterioles of the hamster window model. *Am J Physiol Heart Circ Physiol* 288: H2897–H2903, 2005.
30. **Shibata M, Ichioka S, and Kamiya A.** Estimating oxygen consumption rates of arteriolar walls under physiological conditions in rat skeletal muscle. *Am J Physiol Heart Circ Physiol* 289: H295–H300, 2005.

31. **Sugii Y, Nishio S, and Okamoto K.** In vivo PIV measurement of red blood cell velocity field in microvessels considering mesentery motion. *Physiol Meas* 23: 403–416, 2002.
32. **Sugii Y, Nishio S, and Okamoto K.** Measurement of a velocity field in microvessels using a high resolution PIV technique. *Ann NY Acad Sci* 972: 331–336, 2002.
33. **Torres Filho IP and Intaglietta M.** Microvessel Po_2 measurements by phosphorescence decay method. *Am J Physiol Heart Circ Physiol* 265: H1434–H1438, 1993.
34. **Tsai AG.** Influence of cell-free hemoglobin on local tissue perfusion and oxygenation after acute anemia after isovolemic hemodilution. *Transfusion* 41: 1290–1298, 2001.
35. **Tsai AG, Friesenecker B, Mazzoni MC, Kerger H, Buerk DG, Johnson PC, and Intaglietta M.** Microvascular and tissue oxygen gradients in the rat mesentery. *Proc Natl Acad Sci USA* 95: 6590–6595, 1998.
36. **Tsai AG, Friesenecker B, McCarthy M, Sakai H, and Intaglietta M.** Plasma viscosity regulates capillary perfusion during extreme hemodilution in hamster skin fold model. *Am J Physiol Heart Circ Physiol* 275: H2170–H2180, 1998.
37. **Tsai AG, Johnson PC, and Intaglietta M.** Oxygen gradients in the microcirculation. *Physiol Rev* 83: 933–963, 2003.
38. **Wickramasinghe SR, Lin WC, and Dandy DS.** Separation of different sized particles by inertial migration. *Biotechnol Lett* 23: 1417–1422, 2001.
39. **Wilson DF.** Measuring oxygen using oxygen dependent quenching of phosphorescence: a status report. *Adv Exp Med Biol* 333: 225–232, 1993.
40. **Ye JM, Colquhoun EQ, and Clark MG.** A comparison of vasopressin and noradrenaline on oxygen uptake by perfused rat hind limb, intestine, and mesenteric arcade suggests that it is part due to contractile work by blood vessels. *Gen Pharmacol* 21: 805–810, 1990.